Location-based Resource Allocation for Mobile D2D Communications in Multicell Deployments

Mladen Botsov*, Markus Klügel†, Wolfgang Kellerer† and Peter Fertl‡
*BMW Group Research and Technology, Hanauer Str. 46, 80992 Munich, Germany, Email: mladen.botsov@bmw.de
†Technische Universität München, Arcisstr. 21, 80333 Munich, Germany
Email: {markus.kluegel, wolfgang.kellerer}@tum.de
‡BMW Group, 80778 Munich, Germany, Email: peter.fertl@bmw.de

***Abstract*—Cooperative intelligent traffic systems (C-ITS) will help improve the safety and efficiency of ground transportation by enabling the cooperation between traffic participants. Applications based on the C-ITS paradigm rely on vehicle-to-vehicle, vehicle-to-infrastructure, and vehicle-to-device (collectively, V2X) communication for the exchange of critical information and have very stringent Quality of Service (QoS) requirements on the reliability and availability of the communication links. In order to enable V2X communication using the envisioned device-to-device underlay of future 5G cellular networks, we have introduced a Location Dependent Resource Allocation Scheme (LDRAS) in [1]. In this paper, we enhance and extend LDRAS to multicell deployments, and quantify its performance based on extensive system level simulations. The results show that LDRAS significantly improves the QoS for future C-ITS applications, from radio resource management point of view. However, satisfying the requirements of such services necessitates further improvements of 5G networks over current 4G deployments.**

I. Introduction

A. Motivation

The improvement of traffic safety and efficiency presents the greatest challenge in the transportation of people and goods. Cooperative intelligent traffic systems (C-ITS) [2] are envisioned to contribute towards this goal. Cooperative driving applications, such as platooning or highly automated driving, can reduce travel time, fuel consumption, and CO_2 emissions. Safety services based on the exchange of critical information between vehicles and infrastructure can warn the driver of road hazards as well as actively aid him in avoiding potential accidents. Moreover, the cooperation between vehicles and vulnerable road users (e.g., pedestrians and cyclists) through their mobile devices (e.g., smartphones or smartwatches) could further improve traffic safety. The exchange of messages between vehicles and consumer electronic (CE) devices, however, requires a common communications platform. Such vehicle-to-vehicle, vehicle-to-infrastructure and vehicle-to-device (collectively, V2X) communication could be carried out in cellular networks, as vehicles and CE devices already have built-in cellular modules. However, even the most recent Long Term Evolution (LTE) deployments have been shown to be incapable of satisfying the stringent Quality of Service (QoS) requirements of future C-ITS applications [3].

Part of this work has been performed in the framework of the FP7 project ICT-317669 METIS, which is partly funded by the European Union. The authors would like to acknowledge the contributions of their colleagues in METIS, although the views expressed are those of the authors and do not necessarily represent the project.

B. Device-to-Device Communication for C-ITS

Device-to-Device (D2D) communication has been recently considered as an enabler for new peer-to-peer-based services in future cellular networks [4]. Among other advantages with respect to cellular communication, the D2D paradigm allows for much lower latency, higher throughput and increased spectral efficiency through spatial reuse of radio resources. Moreover, the localized nature of D2D transmissions correlates well with the objective of V2X communication (the exchange between vehicles, infrastructure nodes, and CE devices is only required when they are in close proximity). Hence, D2D communication as an underlay to future 5G cellular networks (i.e., reusing the cellular radio resources) has been identified as a suitable carrier for C-ITS applications [5].

Although D2D communication has been extensively investigated in recent years, the research effort has been foremost focused on static or slowly moving communication partners. The introduction of highly mobile vehicles poses new challenges, especially in regards to radio resource management (RRM). Hereby, many of the state-of-the-art approaches to the RRM problem fail to cope with the fast changing interference conditions and, hence, do not satisfy the QoS requirements of C-ITS. In particular, these requirements include near 100% availability of the communication links and 99.999% reliable transmissions [6]. Hence, a priority in the design of RRM for V2X communications is the stability of the communication system rather than the achievement of high throughput.

C. Contributions of this Work

In an effort to address some of the shortcomings of the state-of-the-art RRM schemes with regards to QoS in mobile D2D communications, we have introduced a Location Dependent Resource Allocation Scheme (LDRAS) in [1]. In this paper we enhance and extend LDRAS to multicell deployments by generalizing the spatial resource reuse strategy and zone design guidelines presented in [1]. Moreover, we apply this approach to an exemplary urban network deployment, and present and discuss its performance based on the results of extensive system level simulations. Hereby, we compare the performance of LDRAS against a selected state-of-the-art reference scheme [7]. Moreover, we quantify the impact of resource reuse in the D2D underlay on the performance of the primary (i.e., cellular) network by comparing to an LTE baseline. We focus our analysis on the reliability and availability requirements of C-ITS applications.

978-1-4673-6305-1/15/$31.00 ©2015 IEEE

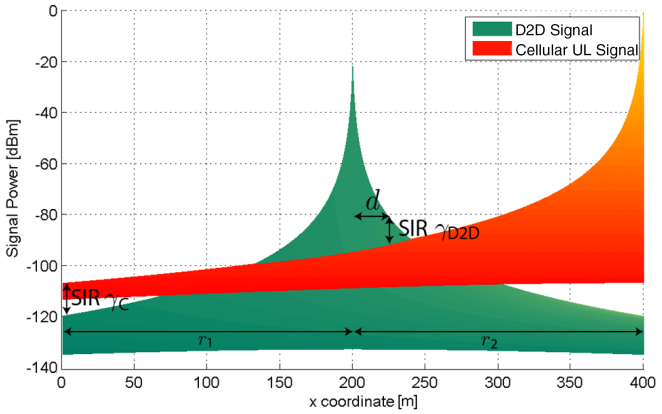

Figure 1. Spatial distribution of the signal power radiated by two transmitters occupying the same radio resources.

II. Location Dependent Resource Allocation Scheme

A. Preliminaries

For the sake of simpler notation and without loss of generality, we assume that the D2D underlay is only available to a certain class of UEs - vehicular terminals (V-UEs) utilizing V2X communications. Hence, the terms *D2D communication* and *V2X communication* are used interchangeably in the context of this paper.

In accordance to the availability requirements of C-ITS applications, the aim of our scheme is to guarantee periodic (or continuous) transmission opportunities for V-UEs in the D2D underlay and at the same time keep the control overhead in the system at a minimum. To this end, LDRAS is built upon a spatial resource reuse scheme and persistent resource allocation tailored to the properties of V2X communication.

B. Spatial Reuse Scheme

The proposed LDRAS reuses the available cellular UL and DL resources for data transmissions in the underlying D2D network. Motivated by the properties of wireless channels we define a resource reuse strategy based on sufficient separation between cellular and D2D users that use the same resources.

1) Reuse of UL resources: First, we focus on the reuse of UL radio resources. Figure 1 shows an example spatial distribution of the signal power radiated by two transmitters exploiting the same UL RBs in the primary network (positioned at $x = 400\,\mathrm{m}$) and in the D2D underlay (positioned at $x = 200\,\mathrm{m}$), respectively. While the maximum transmit power of C-UEs is given by hardware limitations and constraints due to the cell size, the transmit power of V-UEs can be chosen significantly lower as the distances between the UEs in the D2D underlay d are much smaller. For given maximum transmit powers for both UEs, it is possible to achieve predefined Signal-to-Interference Ratio (SIR) targets for (a) cellular communication γ_{C} and (b) D2D communication γ_{D2D} by maintaining certain minimum distances between the evolved NodeB (i.e., base station, eNB) and the interfering D2D transmitter r_1 and between D2D transmitter and C-UE r_2. In this manner, the distance d in which reliable D2D communication is possible can be adjusted according to the requirements of the desired C-ITS services, while also controlling the interference experienced at the eNB. This simple model based on path loss motivates our scheme, but does not take the stochastic nature of wireless channels into account. To this end, we consider the received desired and cross-interference signals in both cases (i.e., in the cases of cellular and D2D communication) to follow the Nakagami distribution [8]. Moreover, we assume worst case cross-interference where all of the interference signals are equally strong and experience similar fading. Following these assumptions, the probability density function (pdf) of the SIR can be expressed as: $f_\gamma(\xi) = \left(\frac{m_S}{R_S}\right)^{m_S}\left(\frac{m_I}{R_I}\right)^{m_t}\frac{\Gamma(m_S+m_t)}{\Gamma(m_S)\Gamma(m_t)}\frac{\xi^{m_S-1}}{\left(\frac{m_S}{R_S}\xi+\frac{m_I}{R_I}\right)^{m_S+m_t}}$. Here, R_S denotes the mean received power of the desired signal, R_I denotes the mean received power from the corresponding interference contributors, m_S and m_I denote the respective Nakagami fading parameter for the desired and cross-interference signals, and m_t denotes the Nakagami fading parameter for the joint cross-interference from multiple sources. Due to space limitations the derivation of the pdf which closely follows the work in [9] is omitted.

Assuming an interference-limited system, reliable communication on a certain link is guaranteed (i.e., the SIR target γ_{t} is met with a certain target outage probability $p_{\mathrm{out,t}}$) when

$$1 - \int_{\gamma_{\mathrm{t}}}^{+\infty} f_\gamma(\xi)\,d\xi \leq p_{\mathrm{out,t}} \tag{1}$$

holds. Evaluating (1) considering the 3 strongest cross-interferers for the case of cellular communication and the 6 strongest cross-interferers for the case of D2D communication yields (2) and (3), respectively. Here, $\overline{PL}(.)$ and $PL(.)$ denote environment-specific path loss models for the links between (a) the interfering V-UEs and the eNB; and (b) the interfering C-UEs and the receiving V-UEs as well as for the link between two V-UEs, respectively. Furthermore, R_0 denotes a certain target Received Signal Strength (RSS) at the eNB enforced by UL power control, $P_{\text{V-UE}}$ the transmit power of V-UEs, and G_0 the maximum eNB antenna gain. $P_{\text{C-UE}}$ denotes the

$$1 - \int_{\gamma_{\mathrm{C}}}^{+\infty}\left(\frac{m_{\mathrm{C}}}{R_0}\right)^{m_{\mathrm{C}}}\left(\frac{m_{\mathrm{D2D}}}{P_{\text{V-UE}}-\overline{PL}(r_1)+G_0}\right)^{3m_{\mathrm{D2D}}}\frac{\Gamma(m_{\mathrm{C}}+3m_{\mathrm{D2D}})}{\Gamma(m_{\mathrm{C}})\,\Gamma(3m_{\mathrm{D2D}})}\frac{\xi^{m_{\mathrm{C}}-1}}{\left(\frac{m_{\mathrm{C}}}{R_0}\xi+\frac{m_{\mathrm{D2D}}}{P_{\text{V-UE}}-\overline{PL}(r_1)+G_0}\right)^{m_{\mathrm{C}}+3m_{\mathrm{D2D}}}}d\xi \leq p_{\mathrm{out,C}} \tag{2}$$

$$1 - \int_{\gamma_{\mathrm{D2D}}}^{+\infty}\left(\frac{m_{\mathrm{D2D}}}{P_{\text{V-UE}}-PL(d)}\right)^{m_{\mathrm{D2D}}}\left(\frac{m_{\mathrm{C}}}{P_{\text{C-UE}}-PL(r_2)}\right)^{6m_{\mathrm{C}}}\frac{\Gamma(m_{\mathrm{D2D}}+6m_{\mathrm{C}})}{\Gamma(m_{\mathrm{D2D}})\,\Gamma(6m_{\mathrm{C}})}\frac{\xi^{m_{\mathrm{D2D}}-1}}{\left(\frac{m_{\mathrm{D2D}}}{P_{\text{V-UE}}-PL(d)}\xi+\frac{m_{\mathrm{C}}}{P_{\text{C-UE}}-PL(r_2)}\right)^{m_{\mathrm{D2D}}+6m_{\mathrm{C}}}}d\xi \leq p_{\mathrm{out,D2D}} \tag{3}$$

maximum transmit power of C-UEs and an isotropic, zero dB gain antenna at V-UEs is assumed.

In order to assure that the inequalities (2) and (3) are always fulfilled, LDRAS relies on cell partitioning. All of the cells in the considered primary network are divided into a total of Z spatially disjoint zones. The available radio resources in each cell are then split into Y resource block (RB) subsets $\mathcal{RB}_y$ ($y = 1, \ldots, Y$) and for each zone z ($z = 1, \ldots, Z$), a specific set of RBs is reserved for D2D communication. The same RB sets $\mathcal{RB}_y$ are then also reused within the primary network. However, here the sets are only allowed to be reused in zones with sufficient spatial separation, as given by r_2, in order to guarantee a certain maximum interference caused by C-UEs in the D2D underlay. Hence, from resource management point of view, a zone is fully described by the tuple $\left(z, \mathcal{RB}_{\text{D2D},z} = \mathcal{RB}_i, \mathcal{RB}_{\text{C},z} \subset \{\mathcal{RB}_y\}_{y=1}^{Y}\right), i \in \{1, \ldots, Y\}$ constructed by the zone index z, the reserved RB sets for D2D communication $\mathcal{RB}_{\text{D2D},z}$, and the set of resources restricted for cellular communication $\mathcal{RB}_{\text{C},z}, \mathcal{RB}_{\text{D2D},z} \subset \mathcal{RB}_{\text{C},z}$, as determined by the neighboring zones of z. Since the cellular UL resources are used in the D2D underlay, any transmitting V-UE within a distance of r_1 from an eNB will cause high interference in the primary network. In order to preserve the reliability of cellular UL transmissions, a dedicated subset of the available UL resources is reserved for the D2D underlay in an area around each eNB (with a radius of at least r_1).

2) Reuse of DL Resources: Similar considerations lead to criteria for the reuse of DL resources analogous to the ones stated in Section II-B1. However, due to space limitations we omit their formulation. The discussion of DL resource reuse is continued in Section III.

C. Resource Allocation Mechanism

Due to the partitioning of the network into zones and the reservation of specific resources, scheduling decisions in the network can be made based on crude position estimation (i.e., only the zone index associated with the considered UE is required to be known).

1) Resource Allocation for V-UEs: We assume that, with respect to the envisioned context awareness of future vehicles, each V-UE is able to use its built-in positioning system in order to track its location within the zone topology. Upon entering a new zone, a V-UE signals the zone index z to the eNB which then assigns a subset of RBs from the appropriate set $\mathcal{RB}_{\text{D2D},z}$ to the V-UE for the entire time it stays in this zone. If the resources in $\mathcal{RB}_{\text{D2D},z}$ are not sufficient to simultaneously serve all V-UEs in zone z, LDRAS instructs concurrent terminals to share specific RBs in time. The availability of resources determines which automotive applications can be supported under given load conditions.

2) Resource Allocation for C-UEs: Resources are assigned to C-UEs in the primary network according to the network operator's scheduling policy, with the additional constraint that RBs from the restricted RB set $\mathcal{RB}_{\text{C},z}$ cannot be allocated to C-UEs in the respective zone z. Assuming that (similar to V-UEs) C-UEs also report their zone index upon entering a new zone, this can be accommodated through a simple modification of the scheduling algorithm. For instance, considering a proportional fair (PF) scheduler [10], the PF metric for all C-UEs in a certain zone z can be altered to an infeasible value (e.g., $-\infty$) in all RBs $\in \mathcal{RB}_{\text{C},z}$. In this manner, it can be ensured that another user in the cell will always be preferred in the considered RBs (see Table I for a minimalistic example).

		PF metric			
C-UE id	z	RB1	RB2	RB3	RB4
C-UE1	1	a	$-\infty$	$-\infty$	b
C-UE2	2	c	d	$-\infty$	$-\infty$
C-UE3	1	e	$-\infty$	$-\infty$	f
Allocation		C-UE1	C-UE2	-	C-UE1

Table I
EXAMPLE BEHAVIOR OF LDRAS-MODIFIED PF SCHEDULER FOR 3 C-UES IN 2 ZONES WITH $\mathcal{RB}_{\text{C},1} = \{\text{RB2}, \text{RB3}\}, \mathcal{RB}_{\text{C},2} = \{\text{RB3}, \text{RB4}\}$, AND PF-METRIC VALUES $a > b > \cdots > f$.

III. ZONE DESIGN AND RESOURCE RESERVATION

The specific zone design depends strongly on the deployment environment and the criteria reflected by the inequalities (2) and (3). Hence, the definition of the zone topology constitutes a multidimensional trade-off spanning the domains of the transmit powers $P_{\text{C-UE}}$ and $P_{\text{V-UE}}$, the desired communication distance d, the spatial separations r_1 and r_2, the SIR targets γ_{C} and γ_{D2D}, and the outage probabilities $p_{\text{out,C}}$ and $p_{\text{out,D2D}}$. The definition of an optimization problem for r_1 and r_2 will be described in a future publication. In the following we work with some fixed feasible r_1 and r_2 and provide additional guidelines on the zone design and resource reservation.

A. Guidelines for Zone Design

The zone design process is initiated by defining an area around each eNB with a radius of at least r_1, where (as motivated above) D2D communication takes place in a dedicated subset of the available UL bandwidth. In order to enable the reuse of radio resources, the rest of each cell has to be partitioned such that the distance between a zone where a certain RB set $\mathcal{RB}_y$ is used in the D2D underlay and at least one additional zone within the same cell is greater than r_2.

The exact size and shape of the individual zones is further influenced by the cell size and the layout of the neighboring zones. We define the neighborhood of zone z as

$$\mathcal{N}_z = \{\forall z' : \text{dist}\,(z, z') \leq r_2, z' \in \{1, \ldots, Z\} \setminus z\},$$

where $\text{dist}\,(\cdot, \cdot)$ denotes the distance between the two closest points in space between the considered zones. Hence, the elements of $\mathcal{N}_z$ induce restrictions on $\mathcal{RB}_{\text{D2D},z}$ and determine $\mathcal{RB}_{\text{C},z} = \{\mathcal{RB}_{\text{D2D},z} \cup \{\mathcal{RB}_{\text{D2D},z'}\}_{\forall z' \in \mathcal{N}_z} \cup \mathcal{RB}_{\text{D2D},\lfloor z \rfloor}\}$; here, $\lfloor z \rfloor$ denotes the zone index of the area within the respective cell sector where D2D communication takes place in a dedicated subset of the UL resources. One of the goals of zone design in this regard is to minimize the cardinality of $\mathcal{N}_z$ in order to relax the constraints for the resource reservation. This can be achieved by increasing the size of the individual zones beyond the minimum given by (3). However, the size of a cell and the necessity to accommodate a sufficient number of zones in it will limit this expansion.

B. Resource Reservation

For a given zone topology, RBs need to be reserved in a fair and efficient way, such that enough resources are available for communication in each zone. Furthermore, in order to ensure that the tolerable interference levels are not exceeded, the following criteria must be met:

a) For each zone z, a subset of the available resources $\mathcal{RB}_{\mathrm{D2D},z}$ has to be reserved for D2D communication, such that the same resources are not used in any of its neighbors for transmissions in the D2D underlay;
b) The resulting sets $\{\mathcal{RB}_y\}_{y=1}^{Y} \setminus \mathcal{RB}_{\mathrm{C},z}$, $\forall z$ should be non-empty to enable cellular communication in each zone.

The size of the different subsets should be chosen according to the expected load in the considered zones.

The above stated reservation problem can be modeled formally with the aid of graph theory [11]. Hereby, the zones in each cell can be interpreted as the set of vertices $\mathcal{V} = \{v_1, v_2, ..., v_{2Z}\}$ in the graph $\mathcal{G} = (\mathcal{V}, \mathcal{E})$. The set of edges $\mathcal{E}$ contains a list of all zone pairs $(v_i, v_j), v_i, v_j \in \mathcal{V}$ that are not allowed to use the same resources according to the above described scheme. Due to the different restrictions for the resource reservation, each geographical zone is represented twice in the graph taking into account the guidelines for (a) D2D and (b) cellular reservation. Graph coloring, commonly used for frequency allocation in 2G cellular networks, provides the required tools for obtaining a valid reservation assignment. The objective is to assign exactly one color to each vertex in the graph corresponding to the requirements for D2D communication and at least one color to each vertex in the graph corresponding to the requirements for cellular communication. This is to be done such that no two vertices connected by an edge have the same color. Assuming that the same amount of resources are required for D2D communication in each zone, each color can be interpreted as a resource block set $\mathcal{RB}_y$. Formally, a valid resource reservation assignment with Y colors is obtained if $\forall v_i, i = 1, \ldots, 2Z, c(v_i) \subset \{1, \ldots, Y\}$ and $\forall (v_i, v_j) \in \mathcal{E}, c(v_i) \cap c(v_j) = \emptyset$; here $c(\cdot)$ denotes the set of colors assigned to the respective vertex. Finding an optimal solution (i.e., a solution using the least possible colors) is quite challenging in practical cell deployments since there are $2Z!$ possible solutions that need to be explored. However, decoupling some of the vertices in the frequency domain (i.e., reserving DL resources for D2D communication in certain zones) helps reduce this complexity and at the same time leads to more efficient reuse of resources. Sequential coloring algorithms [12] can deliver a fast sub-optimal solution. Since satisfactory results can be achieved with a finite amount of trials using random ordered sequential vertex coloring [12] with different permutations of the vertex set, we have adopted this approach in our work.

C. Urban Environment Example

In this paper we concentrate on one of the most relevant deployment environments for the automotive domain - the urban environment. Figure 2 shows one possible example of how the partitioning can be applied to the selected scenario.

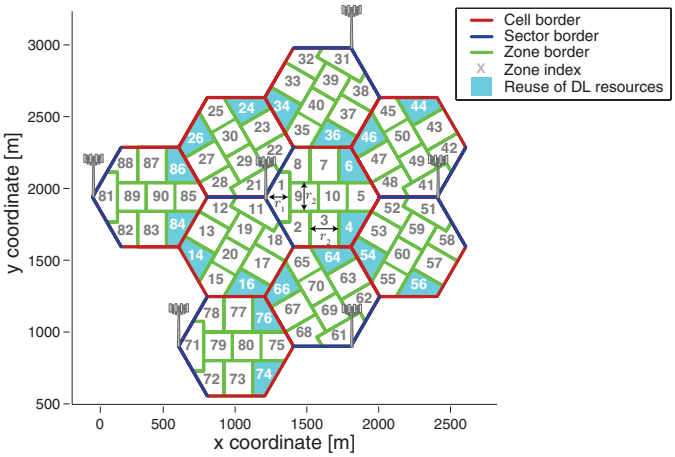

Figure 2. Example zone topology for the considered urban deployment.

Using the parameter values in Table II and the path loss models in Section IV-A, we evaluate the minimal distance between a D2D transmitter reusing UL radio resources and an eNB to $r_1 = 150\,\mathrm{m}$ in order to protect UL transmissions from harmful cross-interference. Similarly, we set the minimal distance between a D2D receiver and a C-UE transmitting in the same resources to $r_2 = 200\,\mathrm{m}$ in order to protect the D2D transmissions from cross-interference. In order to relax the restrictions originating from neighboring relations between the different zones, we allow the reuse of DL in some of the cell edge zones in the topology (marked in cyan).

IV. Simulation Setup

The system performance is determined in terms of the availability, throughput, packet delay and packet error rate in the D2D underlay as well as the throughput in the primary network. As the 5G system is not yet standardized, the computations are based on the LTE Release 9 system specifications, whereas the LTE baseline is extended in order to support D2D communication. Hereby, we introduce the V-UE device class based on the D2D communications paradigm. Note that we realize this without any further modifications to the existing LTE protocol stack (i.e., D2D communication is simulated using the same frame structure, waveform, modulation and coding, etc.) except for the introduction of resource scheduling according to LDRAS. In the primary network, we consider frequency division duplex operation with 100 RBs (or equivalently, a bandwidth of 20 MHz) for either direction, following the LTE orthogonal frequency division multiple access scheme in the DL and single carrier frequency division multiple access scheme in the UL [13]. A portion of the DL and UL resources is reused for D2D communication according to LDRAS, as described in Section III-C. Hereby, the simulated scenario consists of a cluster of 9 cell sectors (as shown in Figure 2), with 54 additional cell sectors generating realistic interference from outside the focus area. Due to performance limitations, these additional sectors are simulated applying the wraparound model and mirror the transmissions from the 9 explicitly simulated sectors. All relevant system parameters reflect realistic LTE deployments and are summarized in Table II.

Parameter	Value
Inter-site distance	1.2 km
Carrier frequency	800 MHz
System bandwidth	20 MHz
eNB antenna height	25 m
UE height	1.5 m
V2X communication distance d	20 m
Cellular SINR threshold γ_{C}	5 dB
D2D SINR threshold γ_{D2D}	7 dB
Cellular outage probability target $p_{\text{out,C}}$	0.05
D2D outage probability target $p_{\text{out,D2D}}$	0.01
Nakagami fading parameter for C-UEs m_{C}	6
Nakagami fading parameter for V-UEs m_{D2D}	4
Shadow fading standard deviation	8 dB
Shadow fading correlation distance	20 m
Maximum eNB antenna gain G_0	14 dBi
eNB horizontal antenna beamwidth	70°
Maximum eNB antenna isolation	20 dB
Vehicular UE transmit power $P_{\text{V-UE}}$	2 dBm
Maximum C-UE transmit power $P_{\text{C-UE}}$	24 dBm
Target RSS at eNB R_0 and at D2D receiver	-85 dBm
Power loss compensation factor α	0.8
eNB noise floor	-117.45 dBm
UE noise floor	-104.5 dBm
Vehicular UE speed	up to 50 km/h
Cellular UE speed	up to 3 km/h

Table II
SYSTEM AND SIMULATION PARAMETERS

A. Path Loss Models, Antenna Gain, and Power Control

The path loss of the links in the primary network as well as for the cross-interference caused by the underlay D2D network in the urban environment is computed according to the WINNER II typical urban macro-cell model [14] (adapted to the considered system model). Hereby, we distinguish between Line-of-Sight (LOS) and Non-Line-of-Sight (NLOS) propagation conditions:

$$\overline{PL}(x) = \begin{cases} 23.06\,\text{dB} + 26\log(x), & \text{LOS} \\ 24.3\,\text{dB} + 35.74\,\text{dB}\,\log(x), & \text{NLOS'} \end{cases}$$

where x denotes the communication link distance (in m). The path loss model for the computation of the signal attenuation between two communicating V-UEs, or between a D2D receiver and the interfering C-UE is based on the WINNER II urban micro-cell model [14]. Hereby, adapting the path loss function to the heights of the UEs in our scenario yields:

$$PL(x) = \begin{cases} 9.31\,\text{dB} + 40\,\text{dB}\,\log(x) \equiv PL_{\text{LOS}}(x), & \text{LOS} \\ \min\left(PL'(d_1,d_2), PL'(d_2,d_1)\right), & \text{NLOS'} \end{cases}$$

where $PL'(d_k,d_l) = PL_{\text{LOS}}(d_k) + 26.01\,\text{dB} - 12.5n_j + 10n_j\log_{10}(d_l)$ and $n_j = \max(2.8 - 0.0024d_k, 1.84)$. The distance d_1 is defined as the separation between the considered UEs in x-direction and the distance d_2 is defined as the corresponding separation in y-direction.

Moreover, for links between eNBs and UEs we consider log-normal distributed shadow fading taken from a 2D correlated fading map using the corresponding parameters from [14]. For the direct links between UEs we consider log-normal shadow fading with a standard deviation of 4 dB.

A 3D antenna pattern is adopted for the calculation of the antenna gain $G(\phi,\theta)$ at the eNBs as follows:

$$G(\phi,\theta) = G_0 - \min\left(25\,\text{dB}, \min\left(25\,\text{dB}, 12\left(\tfrac{\phi}{70^\circ}\right)^2\right) + \min\left(20\,\text{dB}, 12\left(\tfrac{\theta}{10^\circ}\right)^2\right)\right)\ \text{dBi},$$

where ϕ and θ denote the azimuth and elevation angles determined by the positions of the transmitter and receiver, respectively. Isotropic zero dB gain antennas are assumed for the C-UEs and V-UEs.

The transmit power of the C-UEs is calculated by means of fractional power loss compensation, as described in [15]:

$$P_{\text{Tx,C-UE}} = \min\{P_{\text{C-UE}}, R_0 + \alpha L\}.$$

Here, α denotes a power loss compensation factor and L denotes the total power loss measured on the respective link including path loss, shadowing and antenna gain. A similar power control mechanism is also applied to the cellular DL where, according to the restrictions introduced by LDRAS, the transmit power in DL resources used for D2D communication is limited by a threshold of 20 dBm. Allocating such resources to appropriate C-UEs such that the DL performance does not deteriorate is a task of the DL scheduler. In the D2D underlay, V-UEs transmit with a constant transmit power of $P_{\text{V-UE}} = 2\,\text{dBm}$ corresponding to the broadcast nature and desired transmission range of the simulated automotive application.

B. User Traffic and Mobility Models

For the sake of simplicity, we adopt the full-buffer traffic model for all C-UEs in our simulations. At the same time, the application ran by V-UEs is modeled inline with the METIS vision [6]. We define a broadcast-based service (i.e., the transmitted messages are to be received by all V-UEs around the transmitter within the desired broadcasting distance) with a packet size of 1600 bytes and periodicity of 0.67 Hz resulting in a data rate of approximately 8.5 Kbps. The cellular terminals are uniformly distributed throughout the cells while the V-UEs are distributed on fixed roads. The road topology in the urban environment is modeled as a Manhattan grid with a distance of 185 m between adjacent roads in the x-direction and 158.2 m in the y-direction. Realistic movement patterns (including, e.g., waiting at intersections, turning, crossing, etc.) are generated using the Simulator of Urban MObility (SUMO) [16] for speeds of up to 3 km/h for C-UEs (pedestrian behavior) and up to 50 km/h for V-UEs. The positions of all UEs are assumed to be exactly known.

V. SIMULATION RESULTS

Statistical data is gathered in 10 independent simulation runs, each lasting for 60 minutes. The performance of the proposed LDRAS is assessed under medium load conditions, where the number of C-UEs and V-UEs in the network is set to 80 and 320, respectively. Furthermore, we compare the performance of the proposed method to a state-of-the-art reference scheme; in this work, the resource allocation algorithms by Zulhasnine et al. [7] have been selected because of their comparable heuristic nature. In contrast to LDRAS, these algorithms rely on channel state information (CSI) for their decision making. A comparison to the legacy LTE system is also made in order to evaluate the impact of resource reuse on the performance of the primary network. As the cellular traffic is modeled as full-buffer traffic, no QoS requirements

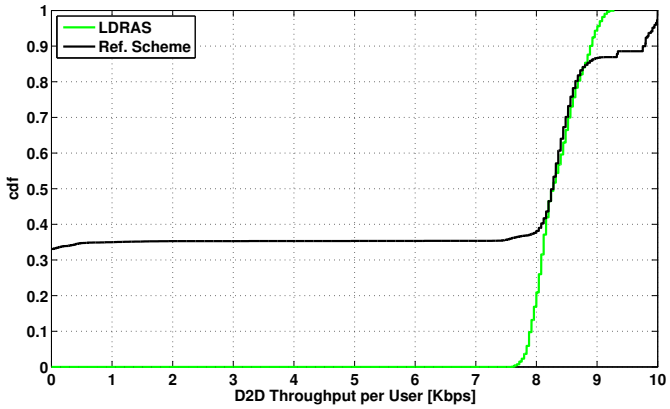

Figure 3. Cumulative distribution function of the measured throughput in the D2D underlay under different RRM algorithms.

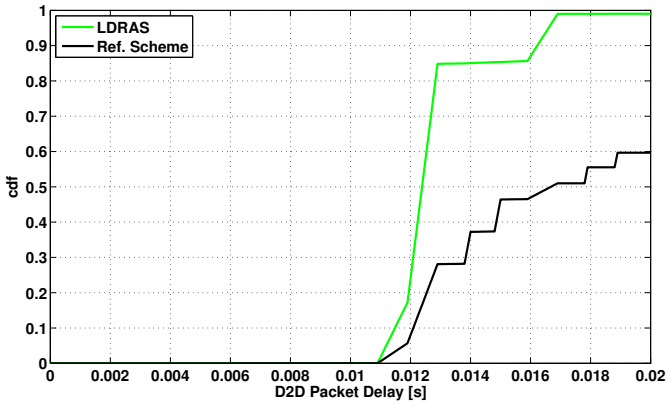

Figure 4. Cumulative distribution function of the measured packet delay in the D2D underlay under different RRM algorithms.

are considered in the primary network. Hence, the analysis focuses foremost on the achieved performance in the D2D underlay and only highlights the impact of resource reuse on cellular communication.

A. D2D Performance

Figure 3 shows the cumulative distribution function (cdf) of the measured throughput in the D2D underlay for all of the considered V-UEs. It can be seen that LDRAS fulfills its design goals and realizes stable performance. A mean throughput of approximately $8.5\,\mathrm{Kbps}$ is achieved, corresponding to the traffic demands in the simulated scenario. In contrast, the reference scheme shows poor reliability (or equivalently, availability) of the D2D links. Due to the opportunistic resource allocation strategy and the prioritization of cellular links, around 40% of the potential vehicular transmissions are dropped as no resources are allocated on time. Note, however, that the reference scheme allows for a slightly higher throughput in certain occasions. This behavior is due to delayed resource allocation such that portions of two packets happen to be considered within the same averaging window.

In addition, Figure 4 shows the cdf of the measured packet delays. Corresponding to the stable performance in terms of throughput, LDRAS results in bounded packet delays. Approximately 85% of the packets are received with a delay of less than $13\,\mathrm{ms}$ and 99% of the packets are received with a delay of less than $17\,\mathrm{ms}$. The "jump" in the cdf is due to waiting times in congested zones where the packet arrival is not synchronized with the resource availability for a portion of the V-UEs. Further note that the packet delay is measured at the Packet Data Convergence Protocol (PDCP) layer and includes processing times (for header compression, segmentation, etc.) of approximately $5\,\mathrm{ms}$ both at the transmitter and at the receiver side. The reference scheme shows similar performance in the occasions where resources are indeed available for D2D communication. Since approximately 40% of the packets are dropped, only the remaining 60% of packets are reflected in the D2D packet delay cdf. Hence, in contrast to LDRAS, the reference scheme fails to offer the required reliability in a mobile D2D communications scenario.

Next, we assess the packet error rate with respect to the distance between a transmitting V-UE and a receiving one (see Figure 5). Here we only focus on the performance of LDRAS. It can be seen that less than 1% of the packets received at a distance below $10\,\mathrm{m}$ from the transmitter cannot be decoded correctly. At the desired broadcast radius of $20\,\mathrm{m}$[1], the packet error rate increases to approximately 2.7%. Indeed, the packet error rate continues to grow exponentially with the distance. For a separation of more than $40\,\mathrm{m}$ between a transmitting V-UE and a receiving one no packet can be decoded error-free. This behavior is determined by the system configuration and can be tuned to match the requirements of a certain C-ITS application up until a certain limit.

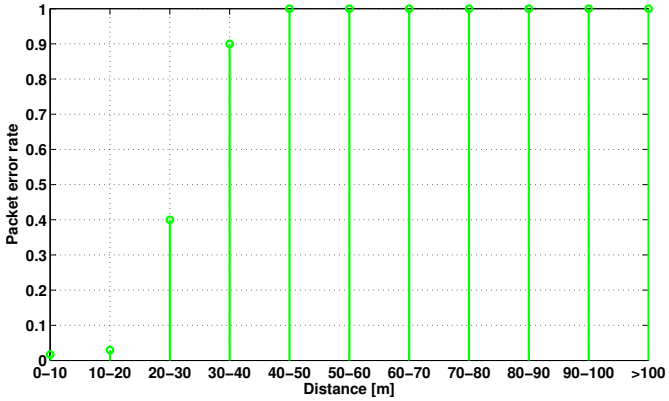

Figure 5. Measured packet error rates under LDRAS at different distances between a receiving V-UE and a respective transmitting one.

B. Impact on the Primary Network

The cdfs of the corresponding throughput in the primary network are shown in Figure 6. Here, we additionally compare the performance achieved with LDRAS and the reference scheme to a legacy LTE system in order to assess the impact of resource reuse. It can be seen that the reuse of DL resources in the D2D underlay has virtually no impact on the cellular links. In fact, LDRAS as well as the reference scheme show almost identical performance with the legacy LTE system. In the UL, on the other hand, both LDRAS and the reference scheme display some degradation compared to the LTE system. Due

[1]V2X broadcast distance of $d = 20\,\mathrm{m}$ is chosen as it would allow for emergency braking in the considered scenario.

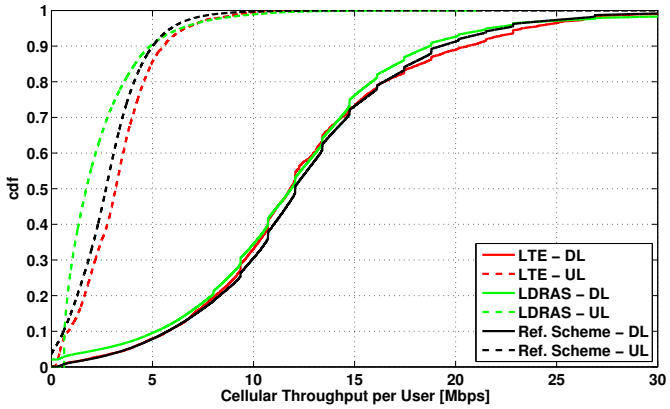

Figure 6. Cumulative distribution function of the measured throughput in the primary network under different RRM algorithms and system configurations.

to the prioritization of cellular links, the performance of the reference scheme is closer to the legacy LTE system. However, this comes at the cost of poor reliability of the D2D links. It should also be noted that a portion of the UL throughput would need to be committed for the acquisition and reporting of the CSI required by the reference scheme. In the case of LDRAS, the mean UL throughput is decreased by 15% as compared to the LTE baseline and by 11% as compared to the reference scheme. The reason for this is two-fold: on one hand, the exclusive utilization of a portion (10% in the simulated example) of the UL resources for D2D communication in close proximity to the eNB leaves less resources for UL transmissions; on the other, the resource reuse and the prioritization of D2D links (required to meet the reliability requirements of C-ITS applications) leads to cross-interference which slightly degrades the UL performance.

C. QoS Analysis with Respect to V2X

Although LDRAS offers significant gains in terms of reliability in the D2D underlay over state-of-the-art RRM approaches, the simulation results show that the improvement of RRM alone is not sufficient to meet the QoS requirements of future C-ITS applications. The METIS project considers packet delay (i.e., end-to-end latency) requirements of below $5\,\mathrm{ms}$ and reliability requirements of 99.999% for V2X communication [6]. As discussed above, the presented packet delay results include a total of $10\,\mathrm{ms}$ of processing time at the transmitting and receiving V-UEs. Hence, in order to meet the requirements for V2X communication, the 5G network needs to introduce a simpler protocol stack and much lower processing times for vehicular services. Subtracting the processing delay, LDRAS shows a transmission delay of less than $7\,\mathrm{ms}$ for 99% of the generated packets, and even as low as $3\,\mathrm{ms}$ for 85% of the generated packets in the considered scenario. The packet delay can be further reduced by increasing the available bandwidth and reducing the transmission time intervals.

Despite the timely D2D transmissions using LDRAS, not all of the intended receiving V-UEs are able to successfully decode the received messages. Aiming for a packet error rate of 0.001% (i.e., setting $p_{\text{out,D2D}} = 1e^{-5}$ while retaining the SINR threshold) would lead to an infeasible zone topology in the considered urban deployment. Hence, the further reduction of the packet error rate (2.7% in Figure 5) at the desired communication distance (i.e., $20\,\mathrm{m}$) would necessitate a redesign of the waveform (allowing for better robustness against non-orthogonal RB usage) or enhanced error correction methods.

VI. Conclusions

In this work, we enhance the LDRAS we proposed in [1] and extend it to multicell deployments. We define criteria and guidelines for the design of the spatial reuse zones and apply graph coloring in order to solve the resource reservation problem. Above all, the aim of LDRAS is to satisfy the requirements of C-ITS safety services (and other applications with similar QoS demands) while reducing the signaling overhead and interference within the primary network. The results of extensive system level simulations show that LDRAS offers significant gains in terms of reliability in the context of mobile D2D communication as compared to state-of-the-art RRM approaches. However, further aspects of the next generation networks need to be enhanced in order to meet the stringent QoS requirements of future C-ITS services.

References

[1] M. Botsov, M. Klügel, W. Kellerer, and P. Fertl, "Location dependent resource allocation for mobile Device-to-Device communications," in *2014 IEEE Wireless Communications and Networking Conference (WCNC)*, April 2014, pp. 1679–1684.

[2] ETSI, "TR 101 607 Intelligent Transport Systems (ITS); Cooperative ITS (C-ITS)," ETSI, Tech. Rep., May 2013.

[3] C. Lottermann, M. Botsov, P. Fertl, and R. Müllner, "Performance evaluation of automotive off-board applications in LTE deployments," in *IEEE Vehicular Networking Conference (VNC)*, Nov. 2012, pp. 211–218.

[4] G. Fodor, E. Dahlman *et al.*, "Design aspects of network assisted device-to-device communications," *IEEE Communications Magazine*, vol. 50, no. 3, pp. 170–177, March 2012.

[5] G. Mange, M. Fallgren *et al.*, "Deliverable D6.2: Initial report on horizontal topics, first results and 5G system concept," ICT-317669 METIS, Deliverable, April 2014. [Online]. Available: https://www.metis2020.com/documents/deliverables/

[6] M. Fallgren, B. Timus *et al.*, "Deliverable D1.1: Scenarios, requirements and KPIs for 5G mobile and wireless system," ICT-317669 METIS, Deliverable, April 2013. [Online]. Available: https://www.metis2020.com/documents/deliverables/

[7] M. Zulhasnine, C. Huang, and A. Srinivasan, "Efficient resource allocation for device-to-device communication underlaying LTE network," in *IEEE 6th International Conference on Wireless and Mobile Computing, Networking and Communications (WiMob)*, Oct. 2010, pp. 368–375.

[8] A. Goldsmith, *Wireless Communications*. Cambridge University Press, Aug. 2005.

[9] J.-C. Lin, W.-C. Kao, Y.-T. Su, and T.-H. Lee, "Outage and coverage considerations for microcellular mobile radio systems in a shadowed-Rician/shadowed-Nakagami environment," *IEEE Transactions on Vehicular Technology*, vol. 48, no. 1, pp. 66–75, Jan. 1999.

[10] S.-B. Lee, I. Pefkianakis *et al.*, "Proportional fair frequency-domain packet scheduling for 3GPP LTE uplink," in *IEEE INFOCOM*, April 2009, pp. 2611–2615.

[11] J. A. Bondy and U. S. R. Murty, *Graph Theory with Applications*. Elsevier Science Publishing, 1976.

[12] F. T. Leighton, "A graph coloring algorithm for large scheduling problems," *Journal of Research of the Notional Bureau of Standards*, vol. 84, no. 6, June 1979.

[13] 3GPP, "TS 36.211 V9 Physical channels and modulation," 2010.

[14] P. Kyösti, J. Meinilä *et al.*, "WINNER II channel models," IST-4-027756 WINNER II, Deliverable, Sept. 2007.

[15] 3GPP, "TS 36.213 V11 Physical layer procedures," 2012.

[16] DLR Institute of Transportation Systems, "SUMO Simulation of Urban MObility," Dec. 2014. [Online]. Available: http://www.dlr.de/ts/sumo/en/